

Evaluation of Visual Pathways in Children with Neuronal Ceroid Lipofuscinosis: Diffusion Tensor Imaging Findings

Hafize Otcu Temur¹, Bahar Atasoy¹, Gözde Yeşil Sayın², Akın İşcan³, Alpay Alkan¹

¹Department of Radiology, Bezmialem Vakıf University School of Medicine, Istanbul, Türkiye

²Department of Medical Genetics, İstanbul University Faculty of Medicine, İstanbul, Türkiye

³Department of Pediatric Neurology, Bezmialem Vakıf University School of Medicine, İstanbul, Türkiye

Cite this article as: Otcu Temur H, Atasoy B, Yeşil Sayın G, İşcan A, Alkan A. Evaluation of visual pathways in children with neuronal ceroid lipofuscinosis; diffusion tensor imaging findings. *Arch Basic Clin Res.* 2024;6(3):177-182.

ORCID iDs of the authors: H.O.T. 0000-0003-0849-0705, B.A. 0000-0002-5393-5876, G.Y.S. 0000-0003-1964-6306, A.I. 0000-0001-5356-2646, A.A. 0000-0002-3002-1641.

ABSTRACT

Objective: The aim of our study is to evaluate whether there were any diffusion tensor imaging (DTI) parameter changes in the visual pathways in children with neuronal ceroid lipofuscinosis (NCL) for the early detection of visual pathway damage.

Methods: Eight patients diagnosed with NCL and 11 controls were included. The fractional anisotropy (FA), apparent diffusion coefficient (ADC), and radial diffusivity (RD) were measured from the visual pathways on DTI. Values of DTI were compared between healthy volunteers and NCL subjects.

Results: There were statistically significant differences in FA, ADC, and RD values obtained from visual pathways in children with NCL. The FA values measured from the occipital lobe at the level of the calcarine cortex were significantly lower in these subjects. The ADC values obtained from the optic chiasm were significantly increased in children with NCL. Also, we detected significantly increased ADC and RD values obtained from the lateral geniculate nucleus and subcortical white matter of the calcarine cortex in NCL subjects.

Conclusion: Optic pathway damage is a core feature in NCL children and the early detection of visual damage is crucial. Therefore, determining the microstructural diffusion changes by using DTI in visual pathways of NCL subjects may provide useful information to understand the underlying pathophysiology of the visual deterioration in NCL and other neurodegenerative diseases.

Keywords: Neuronal ceroid lipofuscinosis, diffusion tensor Imaging, visual pathway, white matter

INTRODUCTION

Neuronal ceroid lipofuscinosis (NCL), also known as Batten disease, is a group of devastating neurodegenerative lysosomal storage disorders. The NCL generally shows generally autosomal recessive inheritance, with disease onset ranging from infancy to adulthood.^{1,2} Epidemiological data indicate an incidence of 1-3/100 000 and a prevalence of about 2-4/1000 000.^{1,3} It is applied to unite the different spectrum of clinical, pathological, and genetic variants, and to date, 14 different NCL phenotypes have been identified.²

The pathogenesis of the NCL is characterized by the accumulation of autofluorescent ceroid lipopigments in the lysosomes and these undegraded products of cellular

metabolism are related with the neurologic autoimmune response, extensive neurodegeneration, and gliosis, which ultimately result in the loss of brain matter and progressive brain atrophy.⁴

All NCL phenotypes are clinically characterized by a combination of symptoms of progressive vision loss, mental and motor deterioration, seizures, ataxia, myoclonus, and premature death.^{1,2,5} For most childhood NCLs, progressive vision loss is the core feature, and ocular pathologies can be the first clinical sign to occur in children and often precede the onset of neurologic dysfunction.

Diffusion tensor imaging (DTI) is an advanced, sensitive technique that has been used to investigate white matter integrity and can provide detection of tissue damage at

Corresponding author: Hafize Otcu Temur, E-mail: hotcutemur@bezmialem.edu.tr



Content of this journal is licensed under a Creative Commons Attribution-NonCommercial 4.0 International License.

Received: July 28, 2023
Revision Requested: June 4, 2024
Last Revision Received: July 14, 2024
Accepted: August 19, 2024
Publication Date: October 15, 2024

the microstructural level that cannot be detected by routine magnetic resonance imaging (MRI).⁶ Previous studies performed with DTI have shown a correlation between DTI data changes and visual deterioration in diverse disorders, including glaucoma, Alzheimer's disease, and mild cognitive impairment.⁷⁻⁹ To our knowledge, there is no study in the literature assessing the DTI features in the visual pathways of NCL subjects yet. Therefore, we aimed to evaluate whether there were any DTI data changes in the visual pathways in children with NCL for the early detection of visual pathway damage.

MATERIAL AND METHODS

The study is a retrospective study approved by the Institutional Ethics Committee of Bezmialem Vakıf University (decision dated October, 02, 2018, numbered 18/236). Eight subjects, who were diagnosed both by phenotypic findings and genetic analysis, participated in this study. Written informed consent was obtained from the participants and their parents who agreed to take part in the study. The 8 subjects (6 male, 2 female, average age 8 years) and 11 age-matched control subjects (4 male, 7 female, average age 11 years) were reviewed. Presenting symptoms were mental and motor deterioration, progressive visual loss, and the seizures. The impairment of vision and the typical ophthalmologic findings were present in all of the children. The patients were those followed by the Department of Pediatric Neurology. The control group consisted of healthy patients who had no clinical history, applied to the outpatient clinic due to headaches, and whose physical examination and MRI were reported as normal. Routine brain MRI and DTI findings of all subjects were evaluated retrospectively.

Magnetic Resonance Imaging Protocol

1.5T MRI system (Siemens, Avanto, Erlangen, Germany) was used with a head coil. First, the conventional MRI protocols comprised T2-weighted turbo spin echo (TR: 2500 ms, TE: 80 ms), FLAIR images (TR: 8000 ms, TE: 90 ms),

and T1-weighted spin echo (TR: 460 ms, TE: 14 ms). The 3D T1-weighted images (TR: 12.5 ms, TE: 5 ms, TI: 450 ms) were acquired by using a magnetization-prepared rapid acquisition of gradient echo sequence (MPRAGE) with an isotropic voxel resolution of 1 mm. Parallel imaging using generalized autocalibrating partially parallel acquisition (GRAPPA) with an integrated parallel acquisition technique (iPAT) factor of 2 was applied. Then the DTI sequences obtained in the axial plane comprised a single-shot, spin-echo, echo-planar sequence with TR: 2700 ms, TE: 89 ms; matrix, 128 × 128; field of view, 230 mm, and slice thickness 5 mm and 30 diffusion-encoding directions were used at b: 0 s/mm² and b: 1000 s/mm². Parallel imaging using GRAPPA with an iPAT factor of 3 was applied. Reconstruction was done using the Leonardo console (software version 2.0; Siemens) for fractional anisotropy (FA), diffusion coefficient (ADC), and radial diffusivity (RD) map. The T1-weighted three-dimensional magnetization-prepared rapid-acquisition gradient-echo and T2-weighted images were used as anatomic references for the placement and tracing of the regions of interest (ROIs) throughout the visual pathway. The ROIs were drawn manually at the size of 3 pixels at the chiasm, 4 pixels at the lateral geniculate nucleus, and 5 pixels at the subcortical white matter of the occipital lobe at the level of the calcarine cortex. The adaptation of the sizes and placement of all ROIs were performed through simultaneous assessment by two experienced radiologists (HOT, BA) on axial color-encoded FA maps based on Dissecting the White Matter tracts: Interactive Diffusion Tensor Imaging Teaching Atlas (Kenichi Oishi, Andreia V. Faria, Peter C M van Zijl, Susumu Mori; MRI Atlas of Human White Matter, 2nd ed.: Academic Press, 2011). To minimize the partial-volume effect, the slices above and below the region were checked to avoid averaging artifacts by examining the conventional images and color FA, ADC map, and diffusion trace side by side in the course of ROI placement.

The FA, ADC, and RD values were measured from the visual pathways on the left side, including optic chiasm, lateral geniculate nucleus, and subcortical white matter at the level of the calcarine cortex (Figure 1A-C). The DTI data measured from the visual pathways of NCL subjects and healthy individuals were compared.

Statistical Analysis

All data were analyzed using Statistical Package for the Social Sciences (SPSS) 17.0 (SPSS Inc.; Chicago, IL, USA), a commercially available software package (SPSS, Chicago, IL, USA). Descriptive statistics were presented with a median (minimum-maximum). The Mann-Whitney *U* test was used to compare FA, ADC, and RD values measured from the visual pathways in children with NCL and

MAIN POINTS

- For most childhood neuronal ceroid lipofuscinosis (NCLs), progressive vision loss is the core feature, and ocular pathologies can be the first clinical sign to occur in children, often precede the onset of neurologic dysfunction.
- Direct assessment of the visual pathway white matter can be accomplished by the use of diffusion tensor imaging (DTI).
- We aimed to evaluate whether there were any DTI data changes in the visual pathways in children with NCL for the early detection of visual pathway damage.

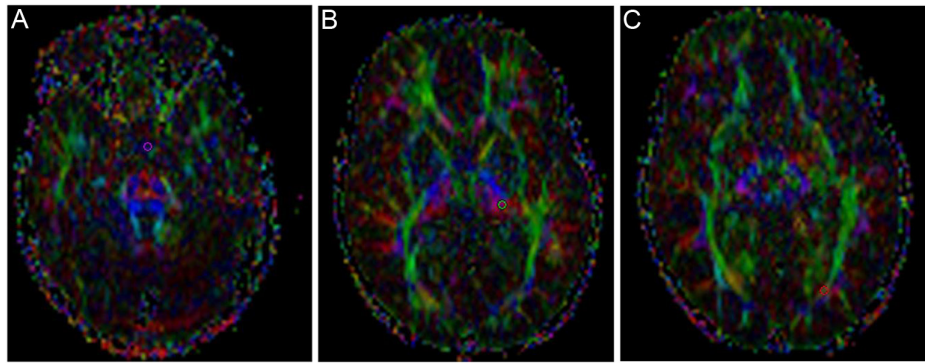


Figure 1. Axial color-encoded FA map demonstrating the placement of the region of interest (ROI) on the optic chiasm (A), lateral geniculate nucleus (B), and subcortical white matter of the calcarine cortex (C).

the control group. P value $< .05$ was accepted to indicate a significant difference.

RESULTS

There were statistically significant differences in FA, ADC, and RD values obtained from visual pathways (optic chiasm, lateral geniculate nucleus, subcortical white matter at the level of the calcarine cortex) in children with NCL compared to the control (Table 1).

The FA values obtained from the subcortical white matter at the level of the calcarine cortex were significantly lower in children with NCL in comparison with controls ($P = .021$).

The ADC values measured from the optic chiasm were significantly increased in children with NCL ($P = .039$). Also, we found significantly increased ADC and RD values obtained from the lateral geniculate nucleus and subcortical white matter of the occipital lobe in NCL subjects.

DISCUSSION

Neuronal ceroid lipofuscinosis is considered the most common form of neurogenetic storage disease in childhood.¹ Due to genetic heterogeneity and the wide phenotypic variability, the characteristics of these symptoms can vary among the NCL forms. Definitive diagnosis of

NCL is made through biochemical enzyme analysis of skin biopsies or blood lymphocytes and mutation detection through molecular genetic studies.^{10,11}

The treatment of NCL is palliative, and to date there is no disease-modifying or curative treatment. As the earliest symptom of most phenotypes of NCL that often refer patients to the physician visual deterioration presents an invaluable chance for intervention before the development of irreversible retinal degeneration. Despite the mechanism underlying visual deterioration in NCL remaining poorly clarified, early diagnosis is crucial for the prevention of irreversible visual changes.

The age of onset of the visual symptoms varies by the NCL phenotypes and generally culminates in total blindness within years. The mechanism underlying vision loss and the pathophysiology of retinal degeneration in NCL remain poorly understood. However, it appears probable that different parts of the optic pathways are affected by the primary defect, and the retinal damage may be triggered by the accumulation of the undegraded granules in the retinal ganglion cells. This may be a primary microglial defect or an upstream insult in the dorsal lateral geniculate nucleus that could promote both optic nerve atrophy and retrograde damage of retinal ganglion cells.¹²⁻¹⁴

The studies demonstrated that the most prominent ophthalmoscopic finding of the CLN3 is the diffuse retinal

Table 1. The FA, ADC, and RD Values Measured on the Optic Chiasm, Lateral Geniculate Nucleus, and Subcortical White Matter of the Calcarine Cortex in NCL Patients and Control Group

	Optik Chiasm		Lateral Genikulat Nucleus		Calcarine Sulcus	
	NCL	Control	NCL	Control	NCL	Control
FA	285 (124-557)	292 (124-557)	354 (240-405)	409 (280-544)	307* (204-362)	368 (248-645)
ADC	1835* (1421-2141)	1422 (1003-2303)	908* (777-1014)	791 (609-865)	1014* (846-1447)	820 (754-919)
RD	1621 (1110-1790)	11196 (735-2152)	703* (645-881)	583 (506-724)	825* (713-1265)	635 (454-735)

ADC, apparent diffusion coefficient; FA, fractional anisotropy; NCL, neuronal ceroid lipofuscinosis; RD, radial diffusivity.

*Statistically significant values $< .05$.

pigment epithelium atrophy of the macula.¹⁵ Pathological examination of the retina has displayed a significant degeneration of the photoreceptors, loss of the outer nuclear layer, accumulation of lipofuscin granules within the retinal pigment epithelium (RPE) and retinal ganglion cells. Despite the injury beginning in the peripheral zone of the retina, in conclusion there's a serious neuronal damage and gliosis throughout the eye.^{13,16}

Recent studies demonstrated that the mouse models of Batten disease (CLN3) have decreased optic nerve axonal density and reduced thickness of myelin.^{13,17} These findings propose that between the retina and higher cortical visual regions, the conduction velocity is declined. Processing of visual data necessitates accurate propagation and segregation of the visual data to the superior colliculus, suprachiasmatic nucleus, and lateral geniculate nucleus (LGN). Disruption in any of these regions negatively affects visual processing and causes damage to the cells either in the retina retrogradely or in the higher cortical visual regions anterogradely, and in conclusion this insult precipitates visual impairment. In addition to that, recent studies suggested that CLN3 proteins play a role in the intracellular motion of amino acids and protein trafficking. Correct protein trafficking is mandatory for accurate communication between the retina and higher cortical visual regions.^{13,18,19} Decreased motion of amino acids from the retina to the LGN suggests retardation of connection between the retina and the projection nuclei. Also, a reduction in the number of large projection neurons within the LGN, which receive input from the retina and transmit it to the visual cortex (V1), was determined in the CLN3 mutant mouse models.¹³ This examination and recent studies suggests that degeneration within the retina is not the main region of insult and the selective cell damage in the LGN could induce both anterograde cell loss within the primary visual cortex and ultimate retrograde damage of retinal ganglion cells.^{20,21}

In NCL subjects, conventional MRI findings included cerebral and cerebellar atrophy, progressive hippocampal atrophy, thalamic signal alterations, and decreased white matter volume in the corona radiata. Conventional MRI is not a sensitive or specific method for early diagnosis. However, it is an excellent tool for objectively monitoring the progression of brain changes.^{2,22} Different imaging findings may occur in different NCL types.^{23,24} The volumetric evaluation of brain volumes by MRI in patients with genetically confirmed CLN2 disease in a recent study revealed a very uniform progression of brain atrophy, strongly related to patient age.²⁵ In another study, in which quantitative measurements of brain volumes were made in patients with infantile neuronal ceroid lipofuscinosis, the volume loss pattern suggests that the order of

involvement is the cerebrum, thalamus, cerebellum, and brainstem, consistent with other previously published studies.²⁶ Increased periventricular white matter signal intensity associated with periventricular loss of myelin and gliosis was revealed in a post-mortem study.²⁷ Decreased gray matter volume in the dorsomedial part of the thalami and related to brain atrophy, diminished size of the corpus callosum is also reported in CLN3.²⁸⁻³⁰ Also in addition to classical neuroimaging findings, abnormal signal intensity was reported in the insular/sub insular region for the first time.³¹

Diffusion tensor imaging is an excellent MRI technique used to assess the structural integration of white matter tracts and to identify pathological changes at the microstructural level, such as axonal or myelin damage. It can provide this information by measuring the magnitude and direction of the diffusion before the insult reaches a level that can be detectable by conventional MRI. All DTI values (FA, ADC, MD, RD, AD) are sensitive to different features of white matter pathology, including maturation, axonal degeneration, and neuronal injury. Especially, FA is highly sensitive to microstructural changes. A decrease in FA values is observed in cases such as white matter disintegration, axonal degeneration, and axonal structural irregularity. On the other hand, it's not so sensitive to the specific type of changes (e.g., radial or axial diffusivity).⁶

A recent study revealed globally decreased FA and increased diffusivity in patients with NCL. In addition, they stated that widespread increased diffusivity and decreased anisotropy, for example, the corona radiata and posterior thalamic radiation. However, they found no differences between the first and second (after 2 years) acquisitions.³²

In this present study, the FA values calculated from the subcortical white matter of the calcarine cortex were significantly lower in NCL subjects. Fractional anisotropy reflects the complex involvement of tissue properties, including the compatibility of fiber orientation, myelination, and axonal density.³³ Decreased FA values in our study can be attributed to axonal degeneration, white matter disintegration, demyelination, and axonal structural irregularity in the visual pathways of children with NCL. We also detected increased ADC values measured from the optic chiasm, lateral geniculate nucleus, and calcarine gyrus. Mean diffusivity or ADC is a sensitive parameter for the assessment of cellularity, edema, and necrosis and is identified as an inverse measure of membrane density.³⁴ Increased ADC values can be associated with microstructural changes such as loss of myelin or local cellular damage in the optic pathways of children with NCL. In addition, we detected significantly increased RD values obtained from the lateral geniculate nucleus, and

calcarine gyrus. Radial diffusivity (RD) is identified as an apparent water diffusion coefficient in the direction perpendicular to the axonal fibers and is a sensitive parameter of demyelination.

The main limitation of our study is the small number of patients. Therefore, the NLC subgroups were not classified.

To the best of our knowledge, this is the first study to determine DTI features of the visual pathways of NCL subjects. While abnormal white matter has been discovered in different brain regions in NCL, there is a lack of imaging data for the visual pathway. Direct assessment of the visual pathway white matter can be accomplished by the use of DTI. Visual damage is a core feature in NCL children and the early detection of visual damage is crucial. Our results suggest that in addition to the retinal cells, higher cortical visual regions are also affected. Diffusion tensor imaging may be useful in clarifying the underlying pathophysiology of visual damage in children with NCL and visual impairment in other neurodegenerative diseases.

Data Availability Statement: The data that support the findings of this study are available on request from the corresponding author.

Ethics Committee Approval: Ethics committee approval was received for this study from the Ethics Committee of Bezmialem Vakif University (Date: 02.10.2018, Approval No.: 18/236).

Informed Consent: Written informed consent was obtained from the participants and their parents who agreed to take part in the study.

Peer-review: Externally peer-reviewed.

Author Contributions: Concept – A.İ., H.O.T., A.A.; Design – A.İ., A.A.; Supervision – A.İ., A.A.; Resources – H.O.T., B.A.; Materials – H.O.T.; Data Collection and/or Processing – H.O.T., G.Y.S.; Analysis and/or Interpretation – H.O.T.; Literature Search – H.O.T., B.A.; Writing Manuscript – H.O.T., B.A.; Critical Review – H.O.T., G.Y.S.; Other – H.O.T.

Declaration of Interests: The authors have no conflict of interest to declare.

Funding: The authors declared that this study has received no financial support.

REFERENCES

1. Simonati A, Williams RE. Neuronal ceroid lipofuscinosis: the multifaceted approach to the clinical issues, an overview. *Front Neurol.* 2022;13:811686. [\[CrossRef\]](#)
2. Kaminiów K, Kozak S, Paprocka J. Recent insight into the genetic basis, clinical features, and diagnostic methods for neuronal ceroid lipofuscinosis. *Int J Mol Sci.* 2022;23(10):5729. [\[CrossRef\]](#)
3. Simpson NA, Wheeler ED, Pearce DA. Screening and epidemiology of Batten disease. *Expert Opinion in Orphan Drug.* 2014;2(9):903-910. [\[CrossRef\]](#)
4. Bozorg S, Ramirez-Montealegre D, Chung M, Pearce DA. Juvenile neuronal ceroid lipofuscinosis (JNCL) and the eye. *Surv Ophthalmol.* 2009;54(4):463-471. [\[CrossRef\]](#)
5. Mole SE, Anderson G, Band HA, et al. Clinical challenges and future therapeutic approaches for neuronal ceroid lipofuscinosis. *Lancet Neurol.* 2019;18(1):107-116. [\[CrossRef\]](#)
6. Alexander AL, Lee JE, Lazar M, Field AS. Diffusion tensor imaging of the brain. *Neurotherapeutics.* 2007;4(3):316-329. [\[CrossRef\]](#)
7. Sidek S, Ramli N, Rahmat K, Ramli NM, Abdulrahman F, Tan LK. Glaucoma severity affects diffusion tensor imaging (DTI) parameters of the optic nerve and optic radiation. *Eur J Radiol.* 2014;83(8):1437-1441. [\[CrossRef\]](#)
8. Mendoza M, Shotbolt M, Faiq MA, Parra C, Chan KC. Advanced diffusion MRI of the visual system in Glaucoma: from experimental animal models to humans. *Biology.* 2022;11(3):454. [\[CrossRef\]](#)
9. Rogojin A, Gorbet DJ, Hawkins KM, et al. Differences in structural MRI and diffusion tensor imaging underlie visuo-motor performance declines in older adults with an increased risk for Alzheimer's disease. *Front Aging Neurosci.* 2023;14:1663-4365.
10. Anderson GW, Smith VV, Brooke I, Malone M, Sebire NJ. Diagnosis of neuronal ceroid lipofuscinosis (Batten disease) by electron microscopy in peripheral blood specimens. *Ultrastruct Pathol.* 2006;30(5):373-378. [\[CrossRef\]](#)
11. Crystal RG, Sondhi D, Hackett NR, et al. Clinical protocol. Administration of a replication-deficient adeno-associated virus gene transfer vector expressing the human CLN2 cDNA to the brain of children with late infantile neuronal ceroid lipofuscinosis. *Hum Gene Ther.* 2004;15(11):1131-1154. [\[CrossRef\]](#)
12. Pontikis CC, Cella CV, Parihar N, et al. Late onset neurodegeneration in the *cln3*^{-/-} mouse model of juvenile neuronal ceroid lipofuscinosis is preceded by low level glial activation. *Brain Res.* 2004;1023(2):231-242. [\[CrossRef\]](#)
13. Weimer JM, Custer AW, Benedict JW, et al. Visual deficits in a mouse model of batten disease are the result of optic nerve degeneration and loss of dorsal lateral geniculate thalamic neurons. *Neurobiol Dis.* 2006;22(2):284-293. [\[CrossRef\]](#)
14. Singh RB, Gupta P, Kartik A, et al. Ocular manifestations of neuronal ceroid lipofuscinoses. *Semin Ophthalmol.* 2021;36(7):582-595. [\[CrossRef\]](#)
15. Hainsworth DP, Liu GT, Hamm CW, Katz ML. Funduscopy and angiographic appearance in the neuronal ceroid lipofuscinoses. *Retina.* 2009;29(5):657-668. [\[CrossRef\]](#)
16. Bensaoula T, Shibuya H, Katz ML, et al. Histopathologic and immunocytochemical analysis of the retina and ocular tissues in Batten disease. *Ophthalmology.* 2000;107(9):1746-1753. [\[CrossRef\]](#)
17. Sappington RM, Pearce DA, Calkins DJ. Optic nerve degeneration in a murine model of juvenile ceroid lipofuscinosis. *Invest Ophthalmol Vis Sci.* 2003;44(9):3725-3731. [\[CrossRef\]](#)
18. Kim Y, Chattopadhyay S, Locke S, Pearce DA. Interaction among Btn1p, Btn2p, and Ist2p reveals potential interplay among the vacuole, amino acid levels, and ion homeostasis in the yeast *Saccharomyces cerevisiae*. *Eukaryot Cell.* 2005;4(2):281-288. [\[CrossRef\]](#)

19. Fossale E, Wolf P, Espinola JA, et al. Membrane trafficking and mitochondrial abnormalities precede subunit c deposition in a cerebellar cell model of juvenile neuronal ceroid lipofuscinosis. *BMC Neurosci.* 2004;5:57. [\[CrossRef\]](#)
20. Marchesi N, Fahmideh F, Boschi F, Pascale A, Barbieri A. Ocular neurodegenerative diseases: interconnection between retina and cortical areas. *Cells.* 2021;10(9):2394. [\[CrossRef\]](#)
21. Mancino R, Cesareo M, Martucci A, et al. Neurodegenerative process linking the eye and the brain. *Curr Med Chem.* 2019;26(20):3754-3763. [\[CrossRef\]](#)
22. Ho M-L, Wirrell EC, Petropoulou K, et al. Role of electroencephalogram (EEG) and magnetic resonance imaging (MRI) findings in early recognition and diagnosis of neuronal ceroid lipofuscinosis Type 2 disease. *J Child Neurol.* 2022;37(12-14):984-991. [\[CrossRef\]](#)
23. Gowda VK, Vegda H, Sugumar K, et al. Neuronal ceroid lipofuscinosis: clinical and laboratory profile in children from tertiary Care Centre in South India. *J Pediatr Genet.* 2021;10(4):266-273. [\[CrossRef\]](#)
24. Johnson AM, Mandelstam S, Andrews I, et al. Neuronal ceroid lipofuscinosis type 2: an Australian case series. *J Paediatr Child Health.* 2020;56(8):1210-1218. [\[CrossRef\]](#)
25. Löbel U, Sedlacik J, Nickel M, et al. Volumetric description of brain atrophy in neuronal ceroid lipofuscinosis 2: supratentorial gray matter shows uniform disease progression. *AJNR Am J Neuroradiol.* 2016;37(10):1938-1943. [\[CrossRef\]](#)
26. Baker EH, Levin SW, Zhang Z, Mukherjee AB. MRI brain volume measurements in infantile neuronal ceroid lipofuscinosis. *AJNR Am J Neuroradiol.* 2017;38(2):376-382. [\[CrossRef\]](#)
27. Autti T, Raininko R, Santavuori P, Vanhanen SL, Poutanen VP, Haltia M. MRI of neuronal ceroid lipofuscinosis. II. Postmortem MRI and histopathological study of the brain in 16 cases of neuronal ceroid lipofuscinosis of juvenile or late infantile type. *Neuroradiology.* 1997;39(5):371-377. [\[CrossRef\]](#)
28. Autti T, Raininko R, Vanhanen SL, Santavuori P. MRI of neuronal ceroid lipofuscinosis: I. Cranial MRI of 30 patients with juvenile neuronal ceroid lipofuscinosis. *Neuroradiology.* 1996;38(5):476-482. [\[CrossRef\]](#)
29. Tokola AM, Salli EK, Åberg LE, Autti TH. Hippocampal volumes in juvenile neuronal ceroid lipofuscinosis: a longitudinal magnetic resonance imaging study. *Pediatr Neurol.* 2014;50(2):158-163. [\[CrossRef\]](#)
30. Autti T, Hämäläinen J, Åberg L, Lauronen L, Tyynelä J, Van Leemput K. Thalamic and corona radiata in juvenile NCL (CLN3): a voxel-based morphometric study. *Eur J Neurol.* 2007;14(4):447-450. [\[CrossRef\]](#)
31. Biswas A, Krishnan P, Amirabadi A, Blaser S, Mercimek-Andrews S, Shroff M. Expanding the neuroimaging phenotype of neuronal ceroid lipofuscinoses. *AJNR Am J Neuroradiol.* 2020;41(10):1930-1936. [\[CrossRef\]](#)
32. Roine U, Roine TJ, Hakkarainen A, et al. Global and widespread local white matter abnormalities in juvenile neuronal ceroid lipofuscinosis. *AJNR Am J Neuroradiol.* 2018;39(7):1349-1354. [\[CrossRef\]](#)
33. Jones DK, Knösche TR, Turner R. White matter integrity, fiber count, and other fallacies: the do's and don'ts of diffusion MRI. *Neuroimage.* 2013;73:239-254. [\[CrossRef\]](#)
34. Feldman HM, Yeatman JD, Lee ES, Barde LHF, Gaman-Bean S. Diffusion tensor imaging: a review for pediatric researchers and clinicians. *J Dev Behav Pediatr.* 2010;31(4):346-356. [\[CrossRef\]](#)